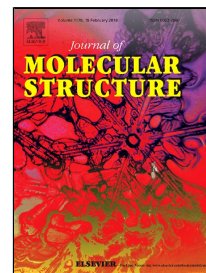


# Accepted Manuscript

Synthesis and Characterization of newly synthesized Schiff base ligand and its metal complexes as potent anticancer



Rania H. Taha, Zienab A. El-Shafiey, Aida A. Salman, Esmail M. El-Fakharany, Mai M. Mansour

PII: S0022-2860(18)31481-9  
DOI: 10.1016/j.molstruc.2018.12.055  
Reference: MOLSTR 25992  
To appear in: *Journal of Molecular Structure*  
Received Date: 19 September 2018  
Accepted Date: 12 December 2018

Please cite this article as: Rania H. Taha, Zienab A. El-Shafiey, Aida A. Salman, Esmail M. El-Fakharany, Mai M. Mansour, Synthesis and Characterization of newly synthesized Schiff base ligand and its metal complexes as potent anticancer, *Journal of Molecular Structure* (2018), doi: 10.1016/j.molstruc.2018.12.055

This is a PDF file of an unedited manuscript that has been accepted for publication. As a service to our customers we are providing this early version of the manuscript. The manuscript will undergo copyediting, typesetting, and review of the resulting proof before it is published in its final form. Please note that during the production process errors may be discovered which could affect the content, and all legal disclaimers that apply to the journal pertain.

*Synthesis and Characterization of newly synthesized Schiff base ligand and its metal complexes as potent anticancer*

Rania H. Taha<sup>a, b\*</sup>, Zienab A. El-Shafiey<sup>a</sup>, Aida A. Salman<sup>a</sup>, Esmail M. El-Fakharany<sup>c</sup> and Mai M. Mansour<sup>a</sup>

<sup>a</sup>Department of Chemistry, Faculty of Science (Girls), Al-Azhar University, P.O. Box: 11754, Yousef Abbas Str., Nasr City, Cairo, Egypt

<sup>b</sup>Chemistry Department, College of Science, Jouf University, P.O. Box: 2014, Sakaka, Saudi Arabia

<sup>c</sup> Protein Research Department, Genetic Engineering and Biotechnology Research Institute (GEBRI), City of Scientific Research & Technological Applications (SRTA-City), New Borg El-Arab City, P.O. Box: 21934 Alexandria, Egypt

\* [rhaly@ju.edu.sa](mailto:rhaly@ju.edu.sa), [mhmd\\_mosad@yahoo.com](mailto:mhmd_mosad@yahoo.com)

### Abstract

2-((2-mercaptophenyl)imino)-1,2-diphenylethan-1-ol(H<sub>2</sub>L) Schiff base ligand from benzoin and 2-aminothiophenol was prepared and characterized. The Co(II), Cd(II), La(III), and Gd(III) complexes were prepared in bulk size and La(III) complex also prepared in nano size. The Schiff base and its complexes were characterized by elemental analysis, <sup>1</sup>H NMR, IR, Mass spectroscopy, UV-VIS spectra, thermal analysis, conductivity measurements, and magnetic moments. The selected analyses showed that the complexes are octahedral and non-electrolytic in nature and the azomethine nitrogen didn't participate in complexation. The ability of the free ligand to remove different heavy metals was studied. The cytotoxicity effect of Cd(II) complex using MTT method exhibited a significant nontoxic behavior and higher cell viability on Vero, Caco-2 and MCF-7 cells than the free ligand itself. The cytotoxicity results revealed that the Cd(II) complex could become safe to be used as anticancer agent for Vero, Caco-2 and MCF-7 cells. By examining its pharmacological activity, we were able to identify new potent and selective anticancer.

**Key words:** Schiff base, aminothiophenol, cytotoxicity, Vero cells, Caco-2 cells and MCF-7 cells

### Introduction

Schiff base ligand is a compound which is prepared by the condensation reaction between aldehyde or ketone with a primary amine [1,2]. The product group is called azomethine group –C=N–. The active groups in the ligand play an important role in its applications. The Schiff base complexes can be prepared by the reaction between the ligand and the metal salts. The Schiff base and its complexes have various applications according to the active groups. They

have applications in industry, pharmacology, biological activities, antimicrobial, antibacterial, anticancer activities, and metallic enzymes preparations [3-9].

Metal complexes of sulphur-containing Schiff bases have received a big attention due to the remarkable antitumor, antibacterial, and antiviral properties.

Schiff base ligand formed from the condensation of benzoin with 2-amino thiophenol and its Co(II), Cd(II), La(III), and Gd(III) complexes were reported in this paper .

### Experimental

Benzoin, 2-amino thiophenol,  $\text{CoCl}_2 \cdot 6\text{H}_2\text{O}$ ,  $\text{CdCl}_2 \cdot \text{H}_2\text{O}$ ,  $\text{La}(\text{NO}_3)_3 \cdot 6\text{H}_2\text{O}$ ,  $\text{Gd}(\text{NO}_3)_3 \cdot 6\text{H}_2\text{O}$ , and ethyl alcohol, etc. were purchased from (Aldrich) and used without purification. The elemental analysis (C,H,N,S) were performed using EL elemental analyser at the microanalytical center, Cairo university, Giza, Egypt. The IR spectra were recorded as KBr discs using a Perkin-Elmer 437 IR spectrometer ( $400\text{-}4000\text{ cm}^{-1}$ ). Mass spectra were recorded at 70 eV and  $300^\circ\text{C}$  on a Hewlett-Packard Mass spectrometer model MS 5988. The proton NMR spectra (DMSO –  $d_6$ ) were recorded on a Bruker FT-400MHZ spectrometer without using internal standard. Electronic (UV – VIS) spectra were recorded on a Shimadzu UV-spectrophotometer in the range (200-800 nm) using (DMSO) solvent. Thermal analyses were carried out using Thermogravimetric analyzer TGA-50 SHIMA VZU and DTA, TA50 Shimadzu in dynamic nitrogen atmosphere with a heating rate  $10^\circ\text{C min}^{-1}$ . The magnetic susceptibility measurements of the complexes were carried out using Gouy balance. The molar conductance was measured on JEN WAY 4510 conductivity meter using DMF as the solvent at room temperature.

### Synthesis of Schiff base ligand

The ligand (1) was synthesized by using the previously published ordinary methods [10]. To the ethanolic solution of benzoin (7.07 g, 0.025 mol) an ethanolic solution of 2-amino thiophenol (3.56 ml, 0.025 mol) was added (1:1 molar ratio), the reaction mixture was refluxed for 4h in a water bath then cooling the reaction mixture. Then the product was collected by filtration, washed several times with ethanol and diethyl ether then dried in a desiccator over anhydrous calcium chloride to give 80.99% yield of Schiff base ligand .

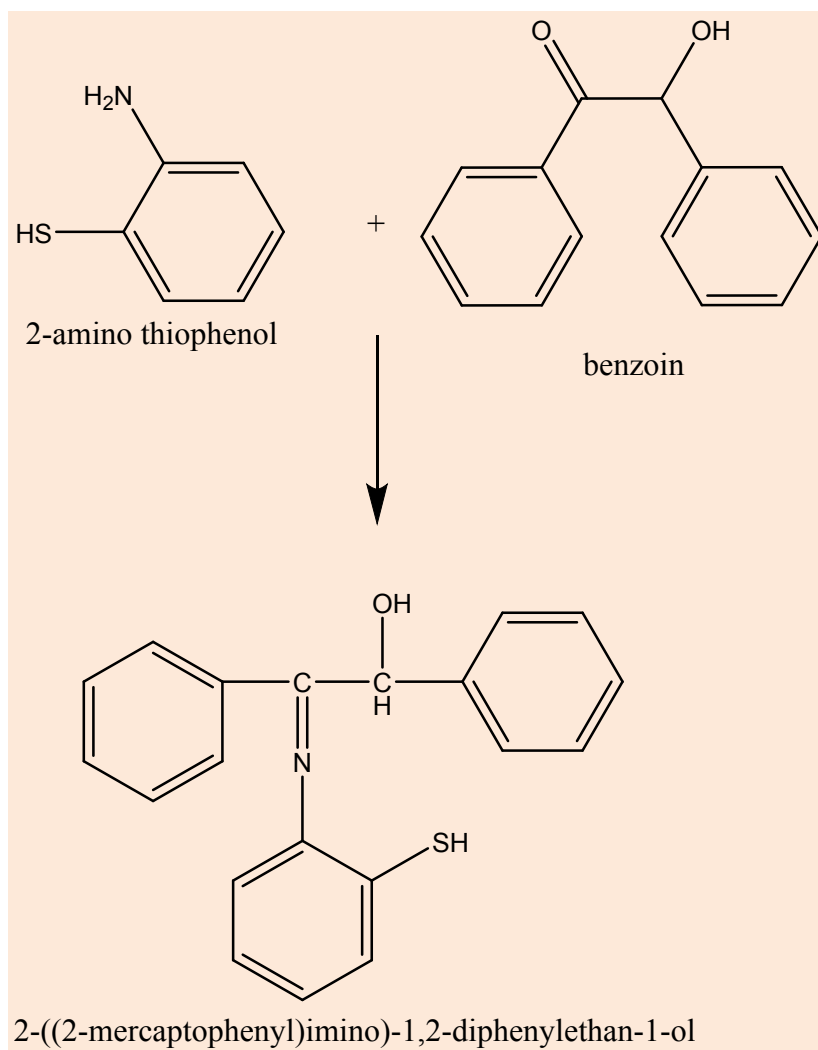


Fig (1): schematic representation of synthesis of bidentate ligand  $H_2L$  .

### Synthesis of metal complexes in bulk size<sup>[11]</sup>

Metal complexes were prepared by adding (0.0025 mol) of ethanolic solution of  $CoCl_2 \cdot 6H_2O$ ,  $CdCl_2 \cdot H_2O$ ,  $La(NO_3)_3 \cdot 6H_2O$ , or  $Gd(NO_3)_3 \cdot 6H_2O$  to a hot solution of Schiff base ligand (0.0025 mol) then the mixture was stirred and reflux for 2 h. The product was collected by filtration, washed with ethanol and diethyl ether then dried in a desiccator.

### Synthesis of La complex in Nano size by green chemistry method<sup>[12]</sup>

10 ml of a 0.1 M solution of  $La(NO_3)_3 \cdot 6H_2O$  in EtOH were positioned in a high-density ultrasonic probe, operating at 24 kHz with a maximum power output of 400 W. Into this solution 10 ml of a 0.1 M solution of the ligands were added drop wise. The obtained precipitate was allowed to evaporate at room temperature to obtain La complex nanoparticle in dark gray powder form.

### Cytotoxicity Assay

Different concentrations of the free ligand and its metal complexes both in bulk and nano size were tested for their cytotoxicity against Vero, Caco-2 and MCF-7 cell lines using (MTT) Thiazolyl Blue Tetrazolium Bromide method according to [13,14]. In brief, Vero, Caco-2 and MCF-7 cells ( $10 \times 10^3$ ) were cultured in a 96 well plate for overnight at 37°C, 5% CO<sub>2</sub> and 88% humidity. The total volume of used DEMEM supplemented medium and the synthesized compounds supernatant was 200  $\mu$ L with final concentrations of 10, 20, 30, 40, 60, 80 and 100 mg/L. The plate was incubated at 37°C, 5% CO<sub>2</sub> for 3 d. After incubation, debris, and dead cells were removed by washing three times with fresh medium. Twenty  $\mu$ L of MTT solution (5 mg/mL of MTT in PBS buffer) was added to each well and shook for 5 min at 150 rpm to thoroughly mix the MTT into the media. The cells were incubated at 37°C and 5% CO<sub>2</sub> for 3-5 h to metabolize MTT by viable cells. 200  $\mu$ L dimethylsulfoxide (DMSO) was added to each well and shook again for 5 min at 150 rpm, and then the viability of the cells was calculated by measuring the optical density at 630 nm subtracted from optical density at 570 nm [15]. The percentage of viability cells was calculated by comparison with control cells (without adding the synthesized compounds to the cells) using the equation of:  $(A)_{\text{test}} / (A)_{\text{control}} \times 100$ .

### Results and discussion

The prepared schiff base ligand and its metal complexes are listed in table (1) together with their elemental analysis data and their physical properties. The elemental analysis data shows that the synthesized compounds have 1:1 (metal:ligand) stoichiometry having molecular formula [Co(H<sub>2</sub>L).2Cl.2H<sub>2</sub>O], [Cd(H<sub>2</sub>L).2Cl.2H<sub>2</sub>O], [La(H<sub>2</sub>L).(NO<sub>3</sub>)<sub>3</sub>.H<sub>2</sub>O], and [Gd(H<sub>2</sub>L).(NO<sub>3</sub>)<sub>3</sub>.H<sub>2</sub>O]. the Co(II), Cd(II), La(III), and Gd(III) complexes have molar conductance 1.87, 1.95, 2.39, and 1.98 S cm<sup>2</sup>mol<sup>-1</sup> representing their non-electrolytic nature [16].

Table (1) : Analytical data and some physical properties of Schiff base ligand , (H<sub>2</sub>L) and its selected metal complexes (1-5)

Molecular formula (M.WT)	colour	M.P (°c)	$\lambda$ m	Elem. Anal .found (calcd. ) %						
				C	H	O	N	S	Cl	M
H <sub>2</sub> L C <sub>20</sub> H <sub>17</sub> NOS (319.38)	Page	114	0.9	75.10 (75.20)	5.22 (5.37)	4.98 (5.00)	4.22 (4.38)	10.12 (10.01)	---	---
(1)[Co(H <sub>2</sub> L)Cl <sub>2</sub> .2H <sub>2</sub> O] CoC <sub>20</sub> H <sub>17</sub> NOS.Cl <sub>2</sub> .2H <sub>2</sub> O (485.25)	Greenish yellow	129	1.87	49.33 (49.49)	4.35 (4.37)	9.75 (9.89)	2.78 (2.88)	6.54 (6.59)	13.98 (14.61)	12.11 (12.14)
(2)[Cd(H <sub>2</sub> L)Cl <sub>2</sub> .2H <sub>2</sub> O] CdC <sub>20</sub> H <sub>17</sub> NOS.Cl <sub>2</sub> .2H <sub>2</sub> O (538.73)	White	250>	1.95	43.99 (44.58)	3.88 (3.93)	8.87 (8.91)	2.57 (2.60)	5.88 (5.93)	13.11 (13.16)	20.65 (20.86)
(3)[La(H <sub>2</sub> L)(NO <sub>3</sub> ) <sub>3</sub> .H <sub>2</sub> O] LaC <sub>20</sub> H <sub>17</sub> NOS.(NO <sub>3</sub> ) <sub>3</sub> .H <sub>2</sub> O (661.43)	Faint brown	135	2.39	36.11 (36.31)	2.87 2.90	26.55 (26.61)	8.44 (8.47)	4.76 (4.83)	---	20.33 (20.86)
(4)[Gd(H <sub>2</sub> L)(NO <sub>3</sub> ) <sub>3</sub> .H <sub>2</sub> O] GdC <sub>20</sub> H <sub>17</sub> NOS.(NO <sub>3</sub> ) <sub>3</sub> .H <sub>2</sub> O (680.68)	Pale green	165	1.98	35.22 (35.28)	2.77 (2.81)	22.89 (23.10)	8.11 (8.23)	4.55 (4.70)	---	22.11 (23.10)
(5)[La(H <sub>2</sub> L)(NO <sub>3</sub> ) <sub>3</sub> .H <sub>2</sub> O] (nano) LaC <sub>20</sub> H <sub>17</sub> NOS.(NO <sub>3</sub> ) <sub>3</sub> .H <sub>2</sub> O (661.43)	page		3.39	36.54 (36.31)	2.83 (2.90)	26.88 (26.61)	8.33 (8.47)	4.55 (4.83)	---	20.99 (20.86)

## <sup>1</sup>HNMR analysis

After having the HNMR analysis we found that the Schiff base ligand fig. (b) give a singlet peak at 10.1 ppm which due to the O-H proton and also give a singlet peak at 3.36 ppm due to S-H proton [17]. In addition to amultiplet peaks at 7.01-8.01 ppm due to phenyl protons. After doing comparison with the metal complex fig.(a) we found that the O-H proton peak shifted to 10.4 ppm and the S-H proton peak shifted to 3.47 ppm and the phenyl protons give a multiplet peak at 7 – 8 ppm. This analysis showed that the O-H and S-H groups share in the complexation with loss of their protons.

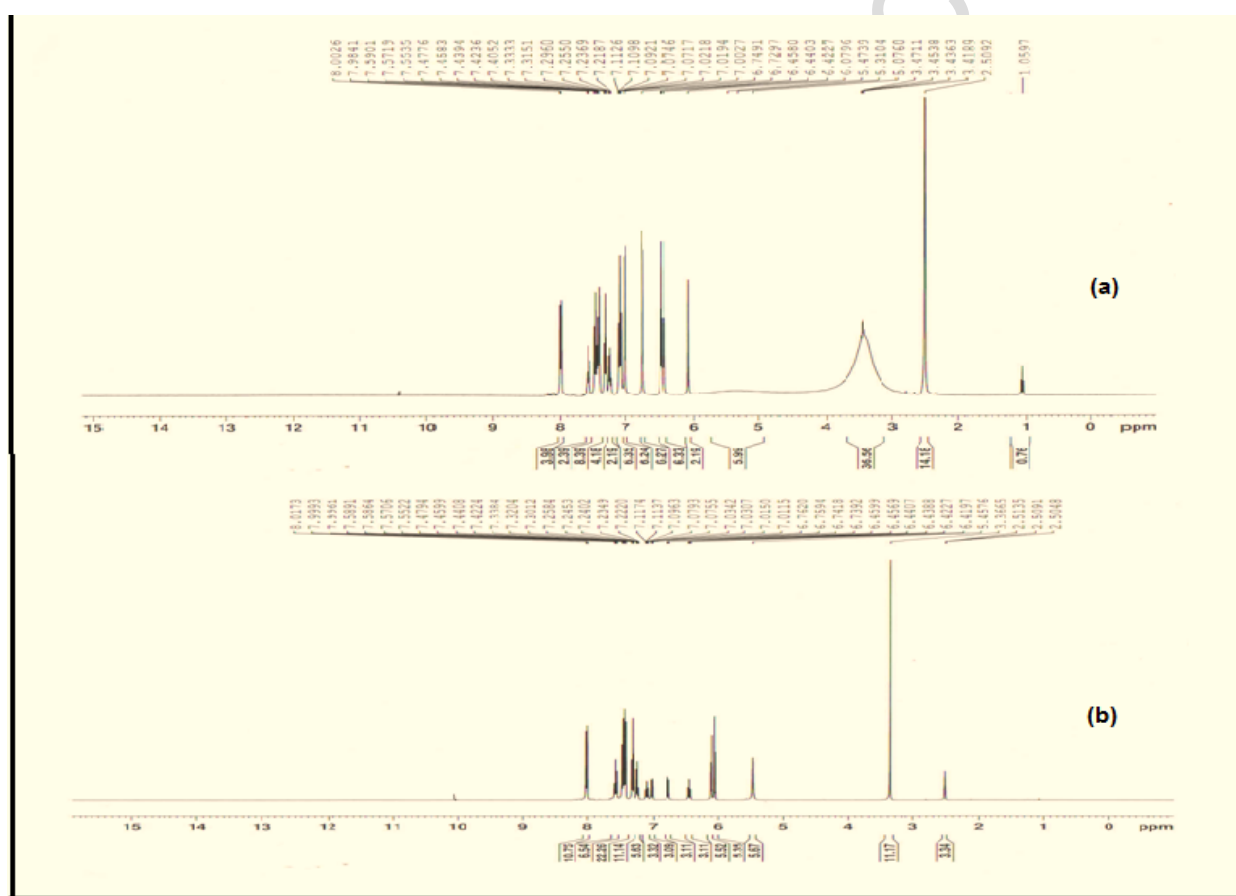


Fig.(2)<sup>1</sup>HNMR spectrum of (a)[Cd(H<sub>2</sub>L)Cl<sub>2</sub>.2H<sub>2</sub>O] complex.

(b) Schiff base ligand H<sub>2</sub>L.

## IR spectra

The IR analysis data listed in table (2). The fig. (3a) showed the IR curve of the Schiff base ligand. The fig. showed the peaks at 3408, 1590, 697, and 1088 cm<sup>-1</sup> due to O-H, C=N, C-S, and C-O groups [18]. The curves.(b-f) showed the IR curves of the complexes.

Table (2) :Significant IR -spectral bands (cm<sup>-1</sup>) of Schiff base ligand , (H<sub>2</sub>L) and its selected metal complexes.

Compd. No.	ν <sub>O-H</sub>	ν <sub>C=N</sub>	ν <sub>C-S</sub>	ν <sub>C-O</sub>	ν <sub>M-S</sub>	ν <sub>M-O</sub>	ν <sub>NO3</sub>		
							ν <sub>1</sub>	ν <sub>2</sub>	ν <sub>3</sub>
H <sub>2</sub> L	3408	1590	697	1088	---	---	---	---	---
[Co(H <sub>2</sub> L)Cl <sub>2</sub> .2H <sub>2</sub> O]	3381	1592	608	1070	512	698	---	---	---
[Cd(H <sub>2</sub> L)Cl <sub>2</sub> .2H <sub>2</sub> O]	3273	1583	605	1162	512	698	---	---	---
[La(H <sub>2</sub> L)(NO <sub>3</sub> ) <sub>3</sub> .H <sub>2</sub> O]	3380	1593	615	1181	479	676	1091	1337	1447
[Gd(H <sub>2</sub> L)(NO <sub>3</sub> ) <sub>3</sub> .H <sub>2</sub> O]	3382	1591	600	1067	510	697	1091	1335	1448
[La(H <sub>2</sub> L)(NO <sub>3</sub> ) <sub>3</sub> .H <sub>2</sub> O](nano)	3380	1593	615	1181	479	676	1091	1337	1447

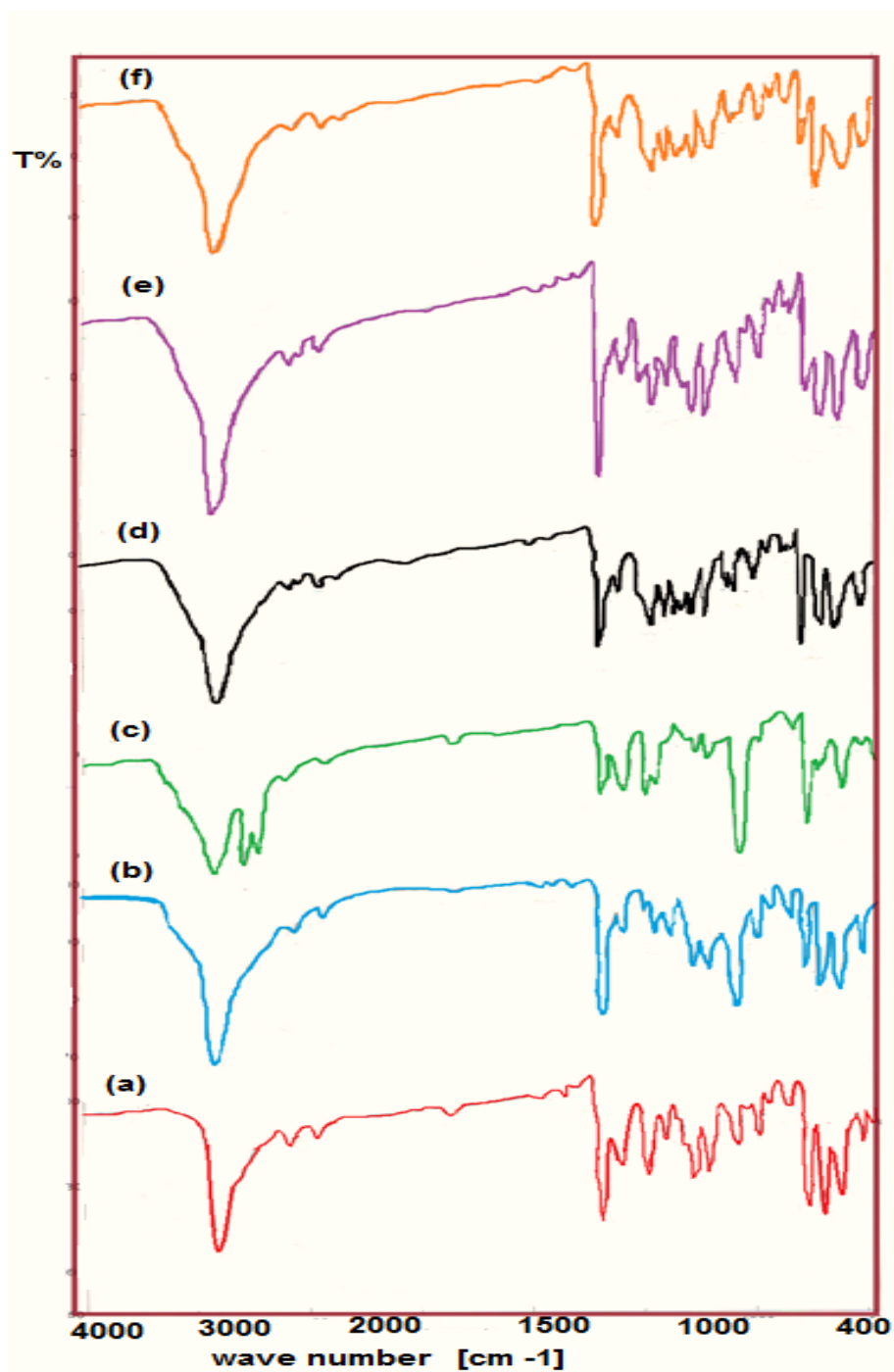


Fig.(3)IR spectrum of:

(a)ligand , H<sub>2</sub>L .(b) [Co(H<sub>2</sub>L)Cl<sub>2</sub>.2H<sub>2</sub>O] .

(c) [Cd(H<sub>2</sub>L)Cl<sub>2</sub>.2H<sub>2</sub>O]. (d) [La(H<sub>2</sub>L)(NO<sub>3</sub>)<sub>3</sub> .H<sub>2</sub>O].

(e) [Gd(H<sub>2</sub>L)(NO<sub>3</sub>)<sub>3</sub>.H<sub>2</sub>O]. (f)[La(H<sub>2</sub>L)(NO<sub>3</sub>)<sub>3</sub> .H<sub>2</sub>O].(nano)

The curves showed that shift in the peaks of O-H, C-O, C-S groups due to their sharing in the complexation and that recorded by the M-O, and M-S peaks. The C=N group doesn't show any shift and this indicate that the azomethine group doesn't participate in complexation.

### Mass spectra

Fig (5) shows the proposed paths of the decomposition steps for ligand .The mass spectrum of free ligand, H<sub>2</sub>L, fig. (4) shows that the peak at m/z 319.86 (11.37%) agree with the molecular formula C<sub>26</sub>H<sub>20</sub>N<sub>2</sub>OS<sub>2</sub>; 319.38. Also, the spectrum shows different peaks corresponding to fragments. Their intensity gives the stability of the fragments.

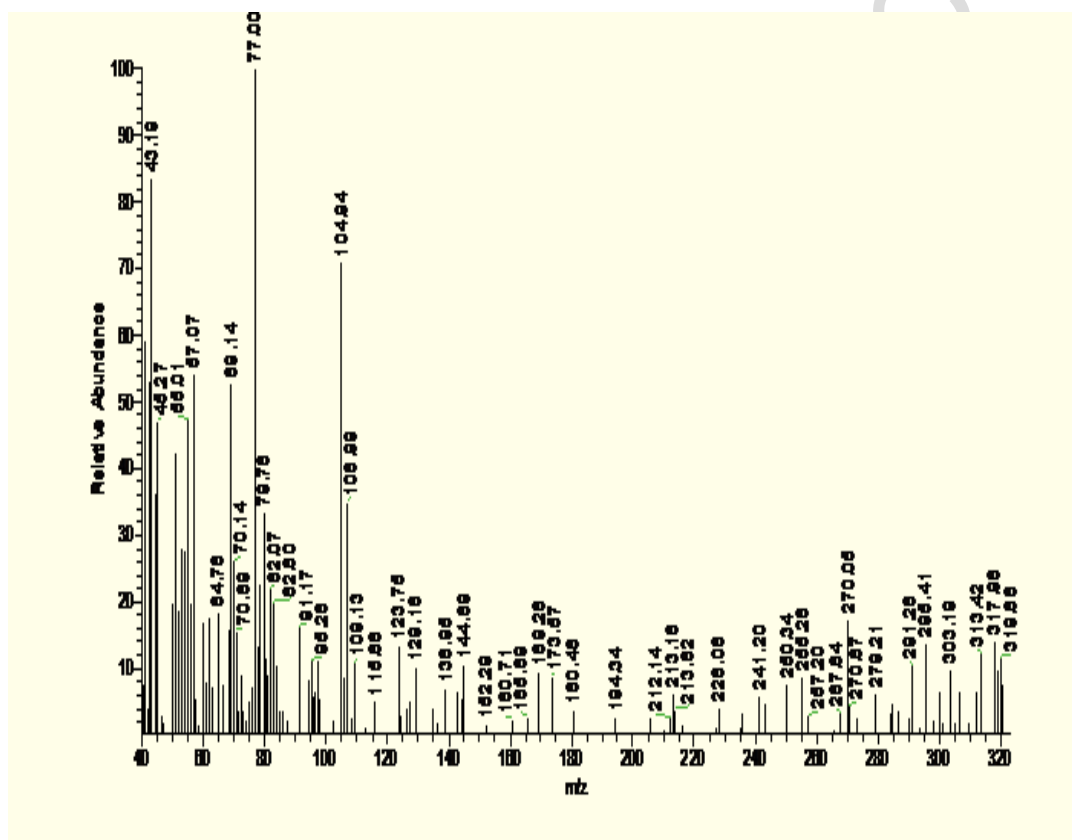


Fig.(4): Mass spectrum of the free ligand H<sub>2</sub>L.

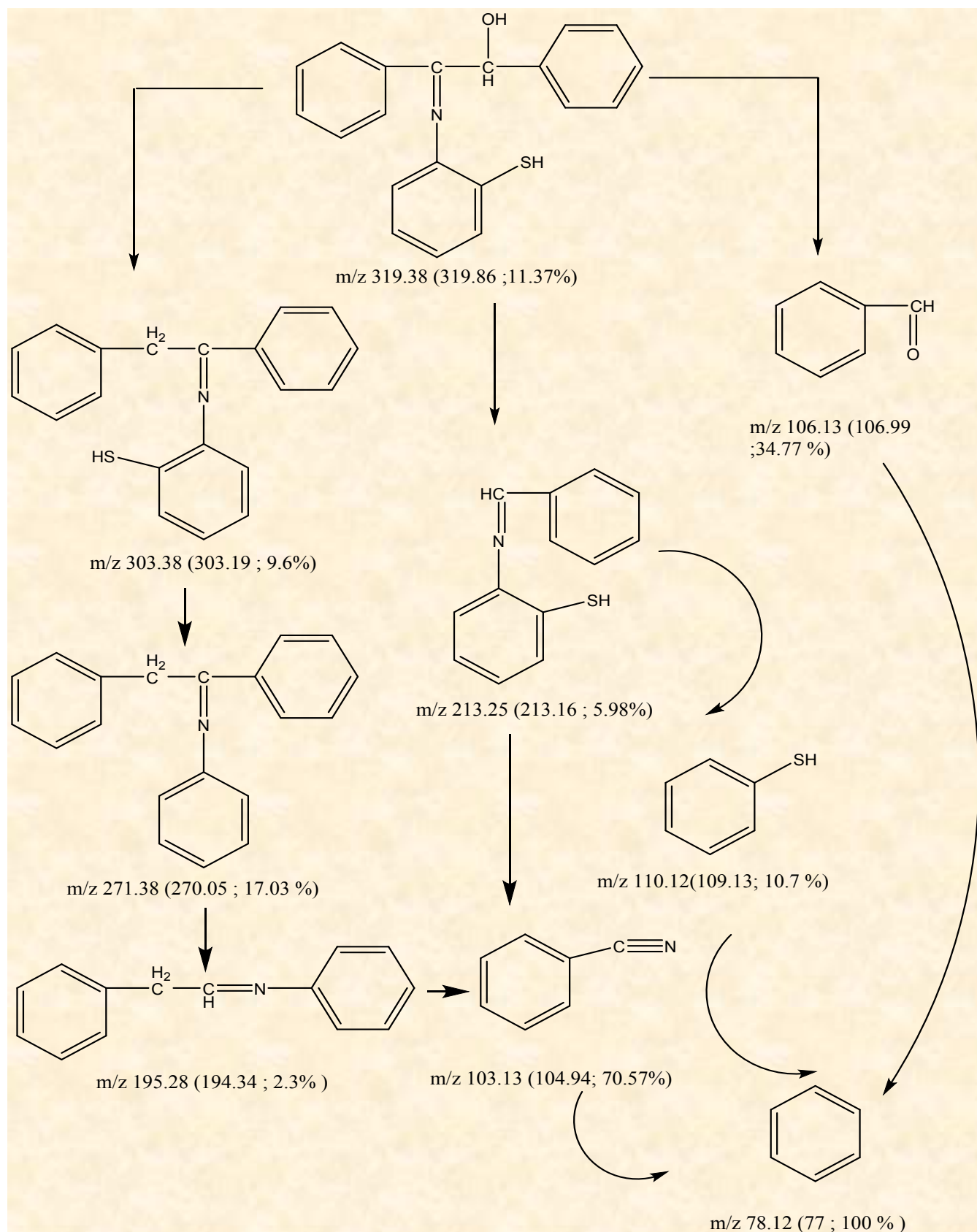


Fig (5): Fragmentation pathway of  $H_2L$  Schiff base free ligand

### UV – vis electronic spectra and magnetic susceptibility measurement

The magnetic moment values and transition bands are listed in table (3), and the electronic spectra of the ligand and its complexes are shown in the fig (6).

The Schiff base ligand shows absorption bands around 282 and 375 nm due to  $\pi \rightarrow \pi^*$  and  $n \rightarrow \pi^*$  respectively. These bands were shifted to another wave numbers on complex formation.

Both Cd(II) and La (III) complexes are diamagnetic in nature with no  $d-d$  transition . The octahedral structure may be suggested according to all previous data and analysis.

The electronic spectra of Co (II) complex showed two absorption bands at 582 and 648 nm assigned to the transition  ${}^4T_{1g}(F) \rightarrow {}^4T_{1g}(P)$  and  ${}^4T_{1g}(F) \rightarrow {}^4A_{2g}(F)$  , and the magnetic moment value is 2.72 B.M. confirmed the octahedral structure .

The electronic spectra of Gd complex have no transition bands over 400 nm because  $f-f$  transition is forbidden. The magnetic moment value is 5.61 B.M. confirmed the octahedral structure [19].

table (3): UV spectra for ligand , H<sub>2</sub>L and its complexes.

Compd. No.	$\mu_{\text{eff}}$ (B.M.)	Absorption bands (nm)		
		$\pi-\pi^*$	$n-\pi^*$	d-d transition
H <sub>2</sub> L	-	282	375	---
1	2.72	210	279	582, 648
2	Diamagnetic	250	309	---
3	Diamagnetic	227	279	---
4	5.61	209	279	---
5	diamagnetic	227	279	---

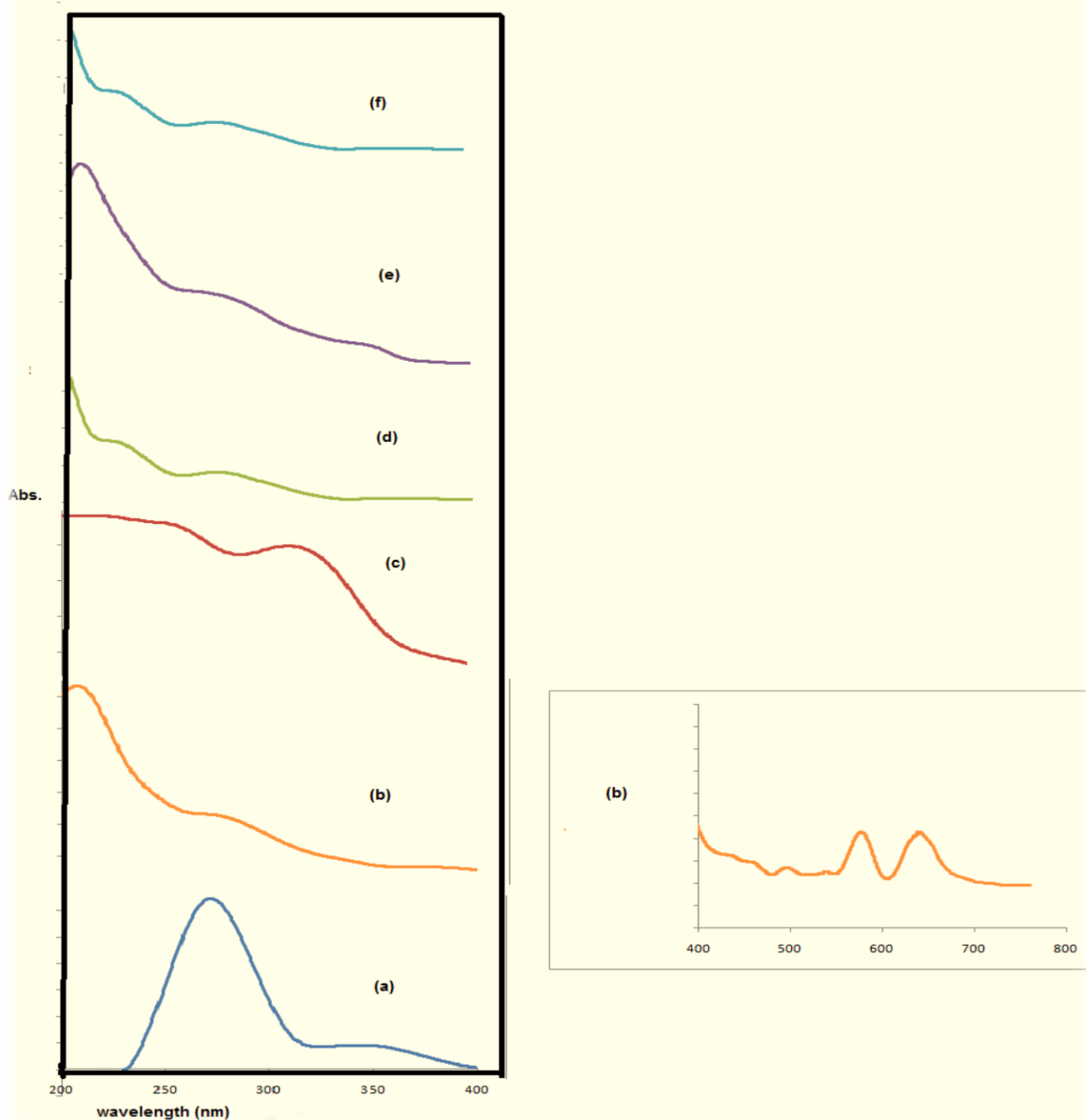


Fig (6): UV spectra for: (a)  $H_2L$  ligand (b)  $[Co(H_2L)(Cl)_2] \cdot H_2O$

(c)  $[Cd(H_2L)(Cl)_2] \cdot H_2O$  (d)  $[La(H_2L) \cdot (NO_3)_2]NO_3 \cdot H_2O$   
 (e)  $[Gd(H_2L) \cdot (NO_3)_2]NO_3 \cdot H_2O$  (f)  $[La(H_2L) \cdot (NO_3)_2]NO_3 \cdot H_2O$  (nano)

### Thermal studies

All data for thermal analysis are listed in table (5). The thermogram of the complex  $[Co(H_2L) \cdot 2Cl \cdot 2H_2O]$ . (fig.7) Shows that there is an water molecule coordinated with metal in the complex. The first stage of decomposition is starting at  $44-198^\circ C$  the observed mass loss

at this stage 2.96 % this due to the loss of water molecule. The second stage of decomposition is from 199<sup>o</sup>C to 421<sup>o</sup>C the observed mass loss is 41.69% this is due to the loss of H<sub>2</sub>O, HCN, H<sub>2</sub>S, Cl<sub>2</sub>, and C<sub>4</sub>H<sub>4</sub>. The third stage of decomposition is from 422<sup>o</sup>C to 574<sup>o</sup>C. The observed mass loss is 10.95% this is due to the loss of C<sub>4</sub>H<sub>5</sub>. The fourth stage is from 575 <sup>o</sup>C to 847<sup>o</sup>C the observed mass loss is 29.40% is due to the loss of C<sub>11</sub>H<sub>5</sub> leaving 14.95% residue as CoO. The overall mass loss is observed to be 85.00% which is in well agreement with the calculated value 84.54%.

The thermogram of the complex [La(H<sub>2</sub>L).(NO<sub>3</sub>)<sub>3</sub> .H<sub>2</sub>O] (fig.8) shows that there is a water molecule coordinated with the metal in the complex . The first stage of decomposition is starting at 43-136<sup>o</sup>C the observed mass loss at this stage 2.29% this due to the loss of water molecule. The second stage of decomposition is from 137<sup>o</sup>C to 239<sup>o</sup>C the observed mass loss is 7.69% this is due to the loss of CO and HCN. The third stage of decomposition is from 239<sup>o</sup>C to 423<sup>o</sup>C. The observed mass loss is 37.42% this is due to the loss of 3HNO<sub>3</sub>, H<sub>2</sub>S, and C<sub>2</sub>H<sub>2</sub>. The fourth stage is from 424<sup>o</sup>C to 596<sup>o</sup>C the observed mass loss is 22.28% is due to the loss of C<sub>10</sub>H<sub>9</sub>. The fifth stage is from 597<sup>o</sup> C to 999<sup>o</sup>C this is due to the loss of La, leaving 10.93 % residue as 6C. The overall mass loss is observed to be 89.06% which is in well agreement with the calculated value 89.07%.

Table (5) :Thermoanalytical results of metal complexes of Schiff base ligand , H<sub>2</sub>L .

Complex compd.	TG range <sup>o</sup> C	Mass loss % obs . (calc.)	Assignment
(1) [Co(H <sub>2</sub> L)Cl <sub>2</sub> .2H <sub>2</sub> O]	44-198	2.96 (3.71)	Loss of H <sub>2</sub> O(coord.)
	199-421	41.69(41.63)	Loss of H <sub>2</sub> O,HCN,H <sub>2</sub> S,Cl <sub>2</sub> and C <sub>4</sub> H <sub>4</sub>
	422-574	10.95(10.94)	Loss of C <sub>4</sub> H <sub>5</sub>
	575-847	29.40(28.26)	Loss of C <sub>11</sub> H <sub>5</sub> , Leaving CoO residue .
		85.04(84.54)*	
(2)[La(H <sub>2</sub> L)(NO <sub>3</sub> ) <sub>3</sub> .H <sub>2</sub> O]	43-136	2.29 (2.72)	Loss of H <sub>2</sub> O (coord.)
	137-239	7.69 (8.31)	Loss ofCO and HCN.
	239-423	37.42(37.65)	Loss of3HNO <sub>3</sub> ,H <sub>2</sub> S ,and C <sub>2</sub> H <sub>2</sub> .
	424-999	22.28(19.53)	Loss of C <sub>10</sub> H <sub>9</sub> . leaving 6C , La metal residue
		69.68(68.21)*	

\*Total Mass Loss

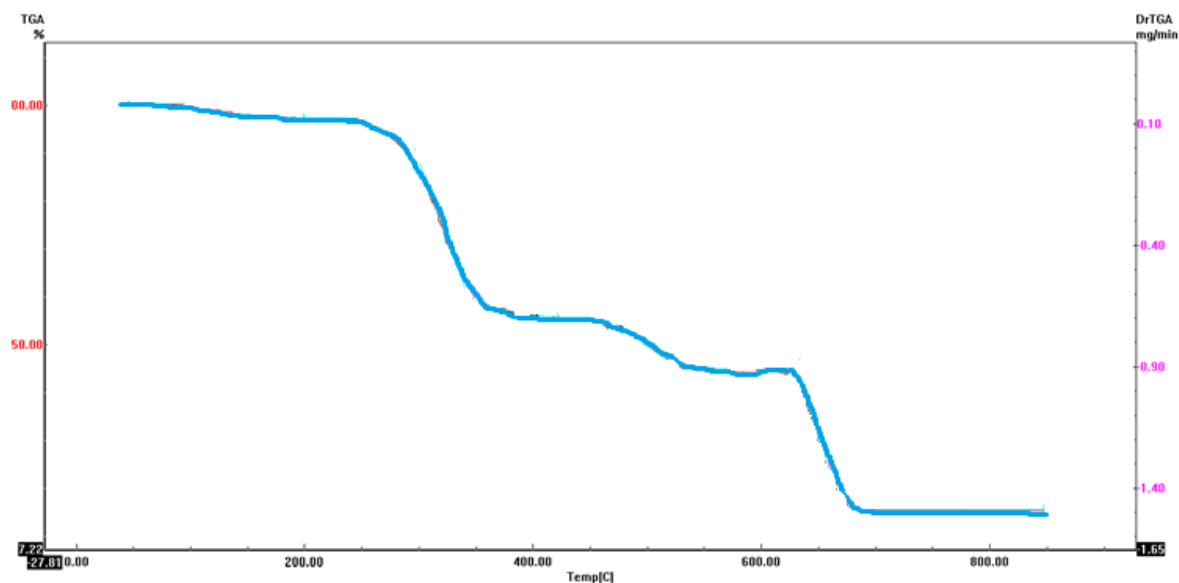


Fig. (7): TGA curve of the  $[\text{Co}(\text{H}_2\text{L})\cdot 2\text{Cl}\cdot 2\text{H}_2\text{O}]$  complex.

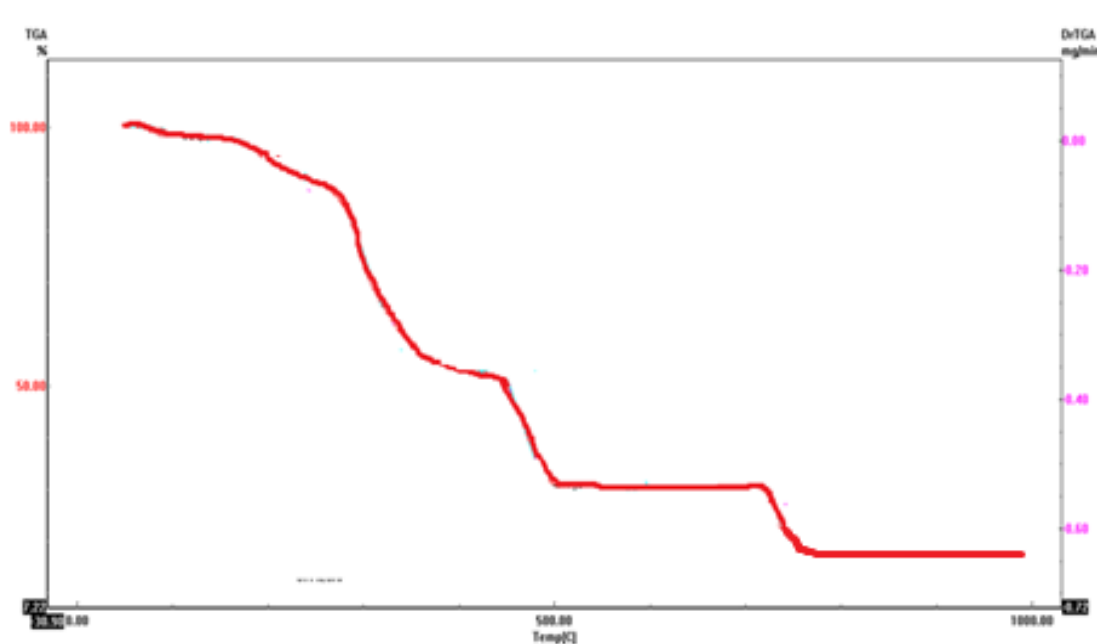


Fig. (8): TGA curve of the  $[\text{La}(\text{H}_2\text{L})\cdot (\text{NO}_3)_3\cdot \text{H}_2\text{O}]$  complex.

#### EDX spectra:

The amount of elements present in percentage level of the metal complexes was identified by EDX data [20]. EDX spectra is used to calculate the percentage level of the elements present in the metal complexes like C, O, N, S and La that present in the La(III) complexes (in bulk and nano size) shown in the fig(9). The revealed data are in good agreement with that of the elemental analysis.

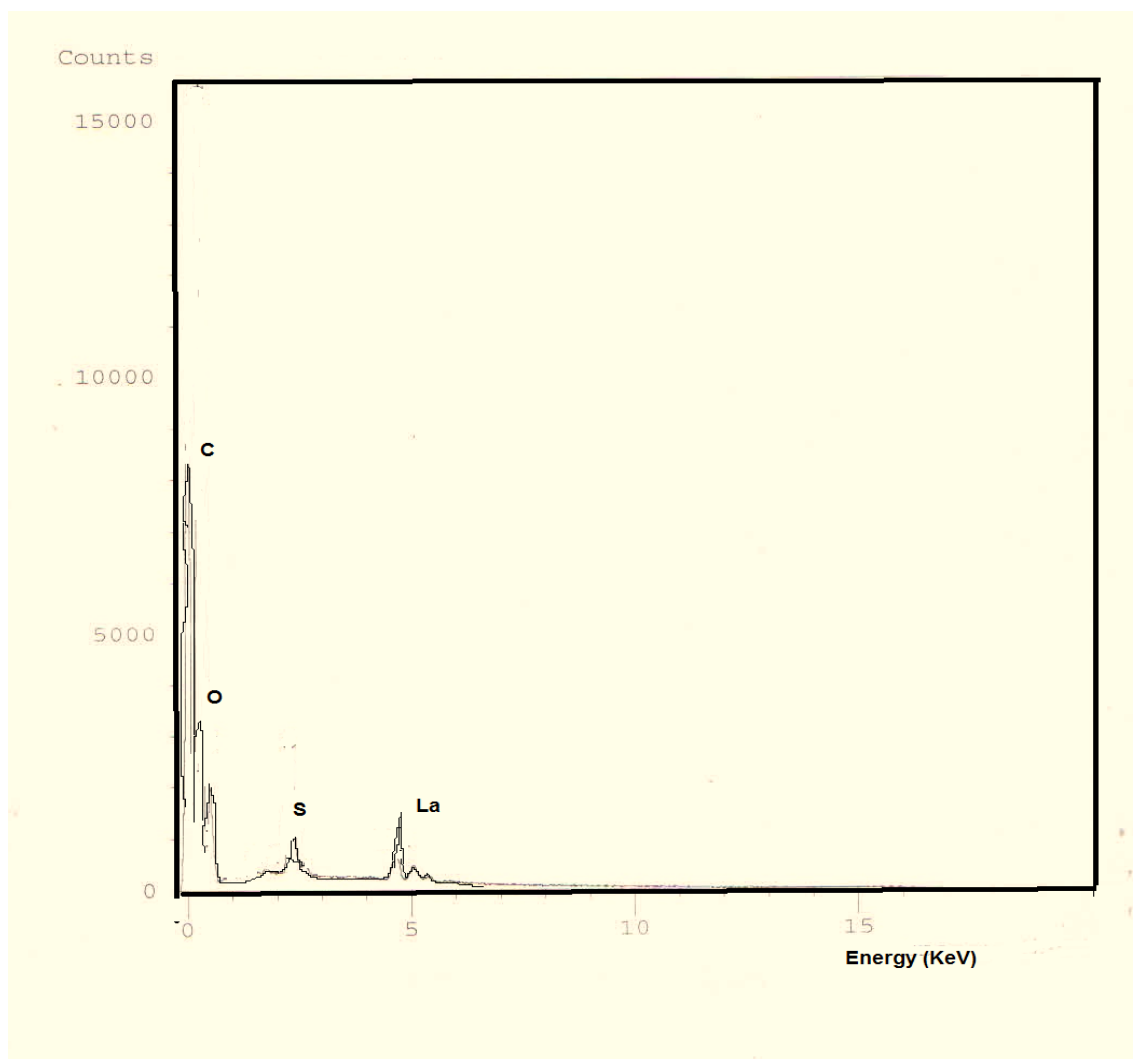


Fig. (9): EDX spectra of La(III) complexes (in bulk and nano size)

Finally, correlation of all techniques used in characterization of the synthesized complexes gives the proposed structure of the metal complexes as represented in Fig. (10).

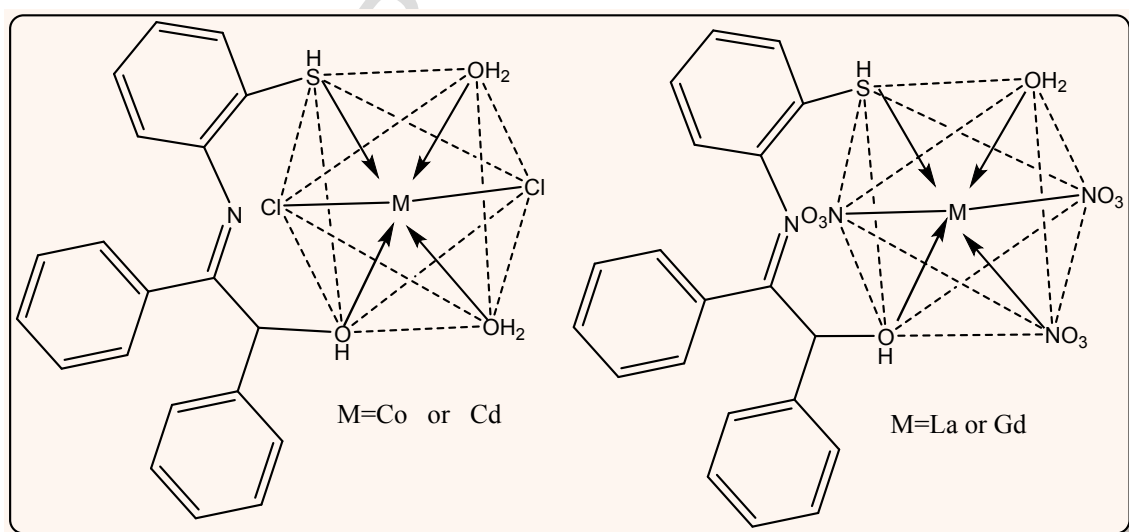


Fig. (10): suggested structure of the complexes

## TEM analysis

Transmission electron microscopy (TEM) can be used to directly image nano particles at scales approaching a single atom. TEM analysis is performed to examine the size and shape of the nano particles. The La(III) complex nano particle was fairly uniform in size, spherical in shape, and with average diameter ranging from 18.66 to 22.68 nm fig. (11). Electron microscopy analysis allowed confirming visually the observed stability of the obtained nano complex.

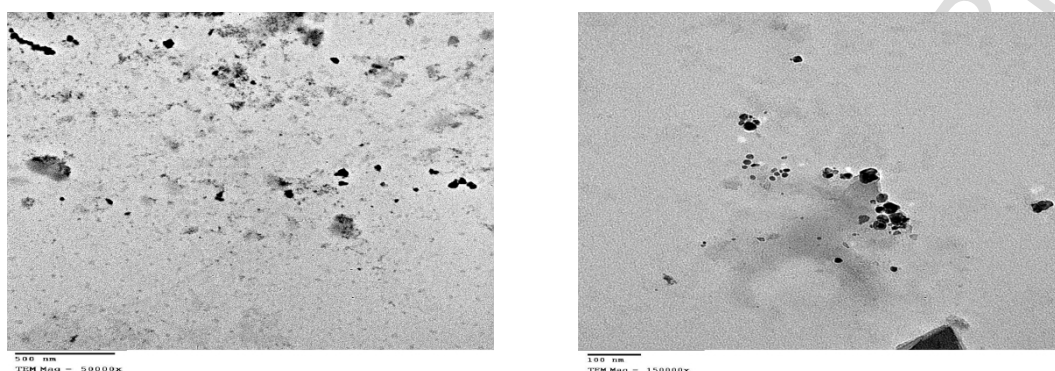


Fig. (11): TEM image of La(III) nano complex

## Metal uptake efficiency of ligand, H<sub>2</sub>L

The important application of the ligand, H<sub>2</sub>L<sup>2</sup> was investigated in removal of Co(II) ions from aqueous solution to detect the optimal contact time effect on adsorption process and to know the maximum elimination capacity of the ligand toward the metal ion under study.

### *Effect of contact time:*

The effect of contact time between the sorbent and the selected metal ions was examined due to detect the appropriate adsorption time. By the variation of the contact time from 0 to 150min for constant dose of the sorbent and constant concentration of the metal ions. It is clear from the result (table 5) fig.(12,13) that as the contact time increases both the removal percentage of the metal ions and adsorption capacity of the ligand increase until equilibrium is attained due to availability of active binding sites on the sorbent. The adsorption process become slower with gradual occupancy of binding sites and finally

reached equilibrium in about 60 min. Further increase in the contact time had a negligible effect on the rate of the adsorption amount. [21].

Moreover, the distribution coefficient  $K_d$  value can be used as a valuable tool to study the metal ion mobility. High values of distribution coefficient indicate that the metal has been retained by the solid phase, while low values indicate that a large fraction of the metal remains in solution [22].

**Table (5):** Capacity study of constant dose of sorbent H<sub>2</sub>L towards Co(II), ions at different contact time

Adsorbed metal ions			
Co(II)			
Contact time (min)	Re %	q <sub>t</sub> (mg/g)	K <sub>d</sub> (ml/g)
15	13.33	37.12	0.0769
30	19.99	55.68	0.1249
45	25.33	70.53	0.16963
60	25.33	70.53	0.16963
75	25.33	70.53	0.16963

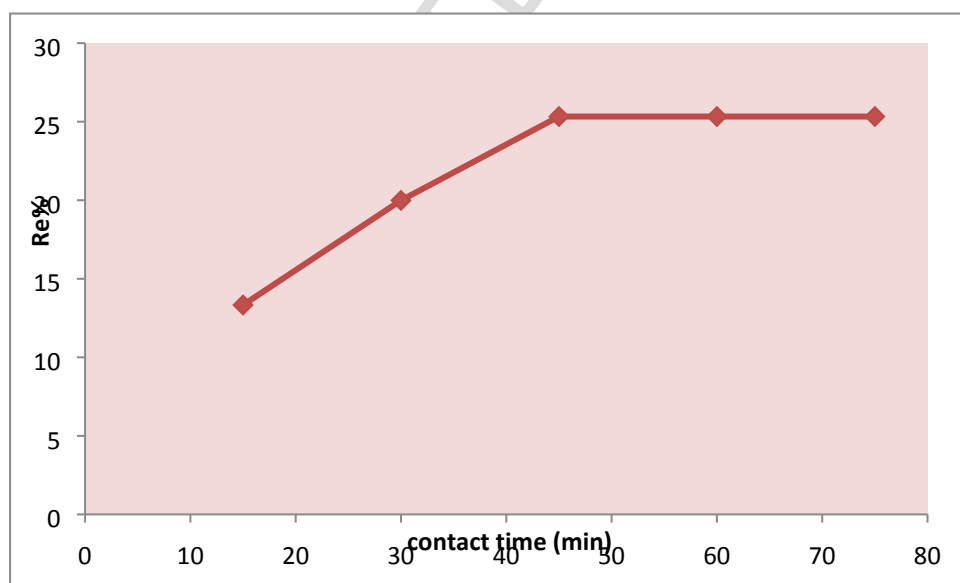


Fig (12): Removal efficiency of the ligand towards Co(II) ions at different contact time

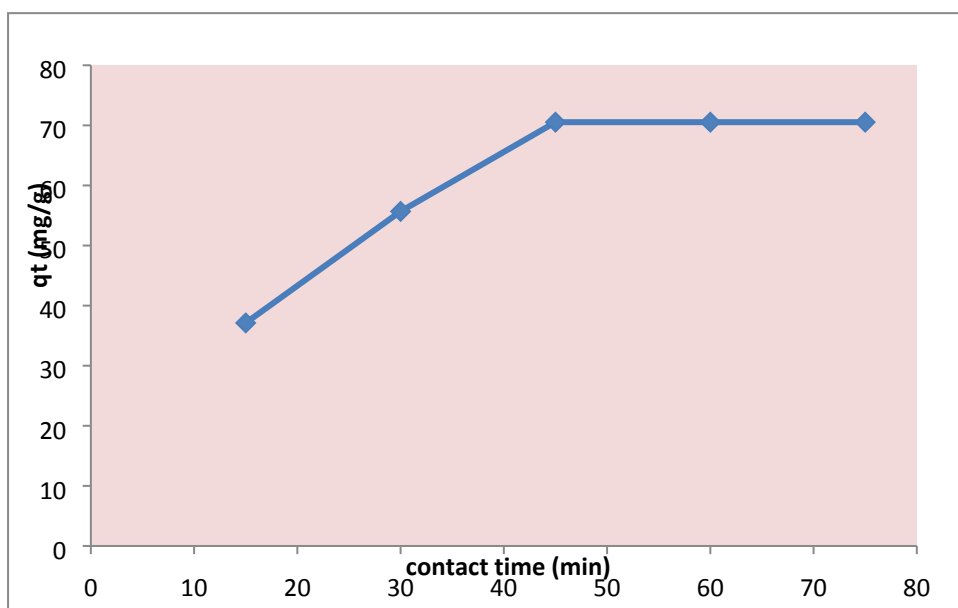


Fig (13): Adsorption capacity of the ligand towards Co(II) ions at different contact time

#### *Effect of adsorbent dose:*

The uptake of the metal ions under study with respect to adsorbent dose was investigated table(6) In order to determine the smallest amount required for maximum removal of metal ions fig(14,15). Experimental results showed that the percentage of metal ions removal increased from 25.33 % to 30.66% for Co(II) ions when the adsorbent dosage increased from 0.1 to 0.3gm. This may be due to the more adsorption sites available for the metal ions. Also, the adsorption capacity was increased when the adsorption dosage increased due to the saturation of adsorption sites as a result to the increase in adsorbent amount and a constant metal ion concentration and constant volume. Also, this increase in capacity may be due to the increase in total surface area of the adsorbent.

**Table (6):** Effect of different doses of sorbent on the adsorption of Co(II), ions at equilibrated contact time

Different doses of H <sub>2</sub> L ligand as sorbent at equilibrated contact time						
	0.1gm		0.2gm		0.3gm	
Adsorbed metal ions	Re %	q <sub>t</sub> (mg/g)	Re %	q <sub>t</sub> (mg/g)	Re %	q <sub>t</sub> (mg/g)
Co(II)	25.33	70.53	28	38.98	30.66	28.46

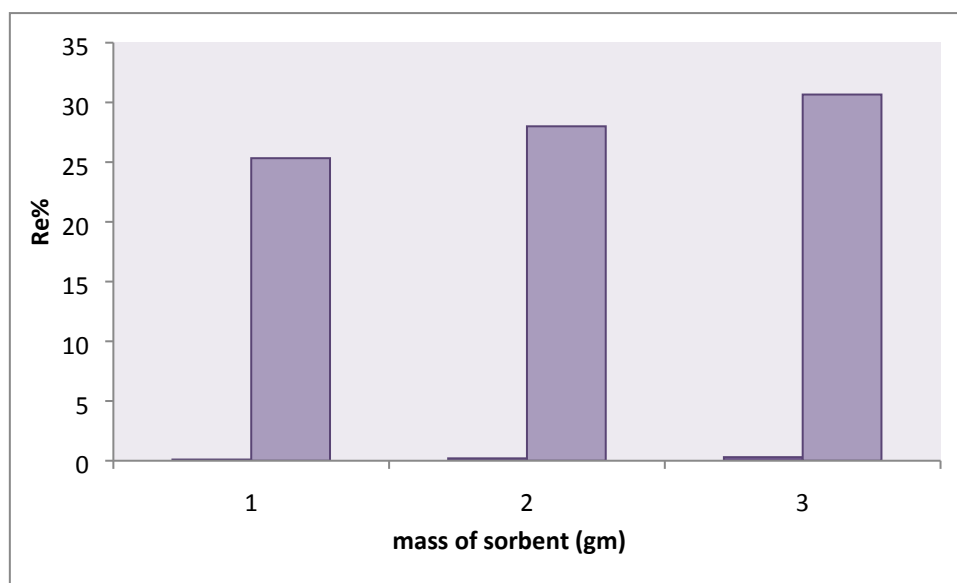


Fig (14): Removal efficiency of the sorbent dosage towards Co(II) ions

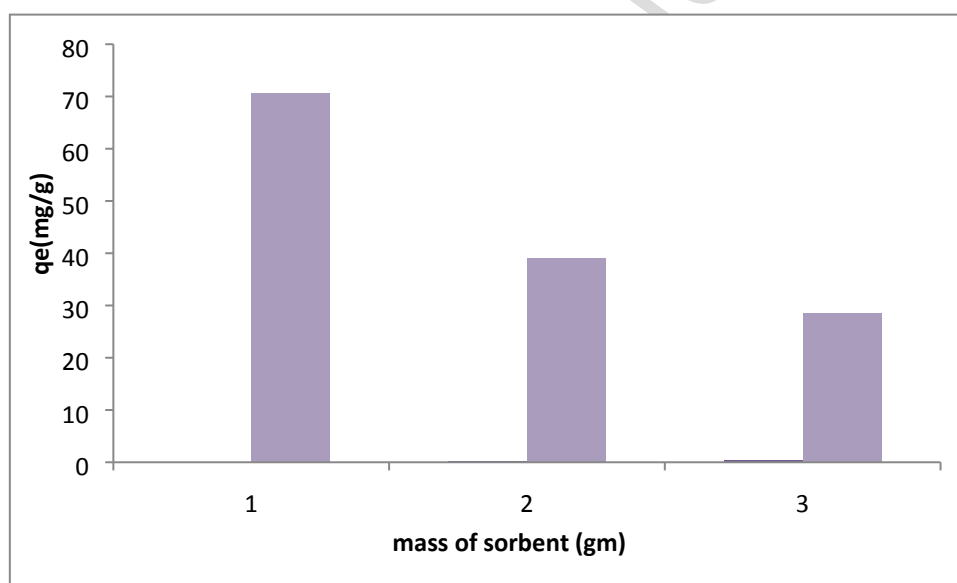


Fig (15): Adsorption capacity of the sorbent dosage towards Co(II) ions

***Effect of different concentrations of metal ions at equilibrated contact time and specific weight of ligand***

In order to determine the removal activity of the sorbent with increase in the metal ion concentrations, the uptake of the metal ions under study with respect to specific adsorbent dose was investigated table(7) fig(16,17). Experimental results showed that the percentage of metal ions removal decreased when the metal ion concentrations decreased from 0.03 to

0.003gm. Also, the adsorption capacity was increased when the metal dosage increased due to the saturation of adsorption sites as a result to the increase in metal ion concentration[23].

**Table (7):** Effect of different concentrations of metal ions at equilibrated contact time and specific weight of ligand.

Adsorbed metal ion	0.003 M/L		0.005 M/L		0.01 M/L		0.02 M/L		0.03 M/L	
	Re %	$q_e$	Re %	$q_e$	Re %	$q_e$	Re %	$q_e$	Re %	$q_e$
Co(II)	25.86	55.09	27.27	66.83	25.33	70.53	26.71	129.94	34.59	237.6

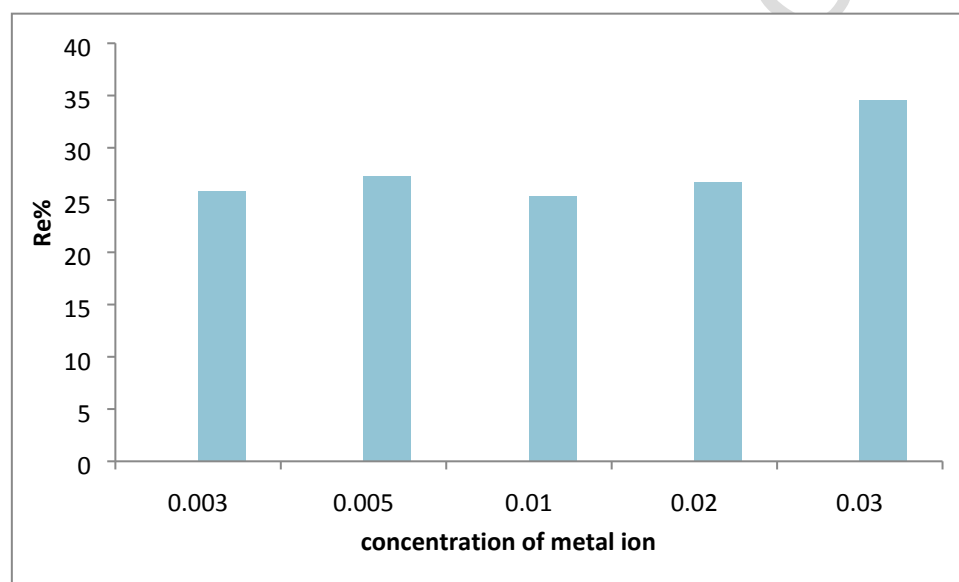


Fig (16): Removal efficiency of the sorbent dosage towards different concentrations of Co(II) ions

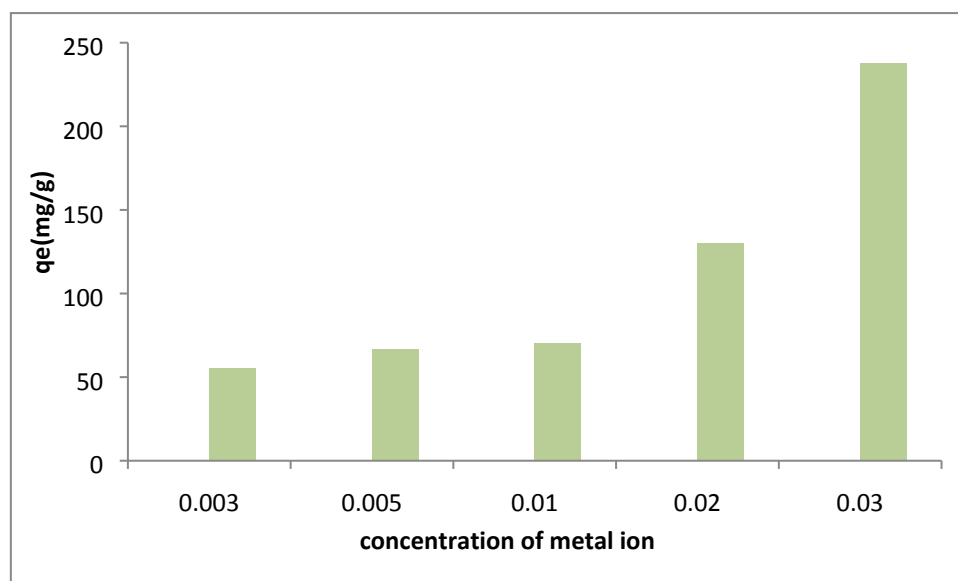


Fig (17): Adsorption capacity of the sorbent dosage towards different concentrations of Co(II) ions

### **In vitro Cytotoxicity Effect on Mammalian Cells**

The cell viability (%) was investigated in vitro by MTT-assay using Vero, Caco-2 and MCF-7 cell. As given in Figs. (18, 19, 20), the free ligand did not exhibit any cytotoxicity on the cells and the cell viability was around 100(%) for all lower used concentrations. While on higher concentrations the cell viability was around 90-70(%)

### **Cytotoxicity Effect of the selected metal complexes on Mammalian Cells**

The cytotoxicity effect of the selected metal complexes was assayed using MTT assay test. It was shown from tables (8, 9, 10) that while the free ligand did not exhibit any activity, upon complexation the activity increased. The cd(II) complex show the best cytotoxicity effect on all cells and reduced the cell viability to become 6%, 7.8% and 12% for Vero, Caco-2 and MCF-7 cell, respectively. Then the La(III) complex which show the viability of Vero, Caco-2 and MCF-7 cell to be 14, 26 and 27% respectively. Additionally, the relative activities of the Co(II) complex on the viability of the Mammalian cells at were reported to be 71, 75 and 61%, respectively.

Table (8) : Cytotoxic effect of free ligand and its metal complexes on the viability of Vero cells

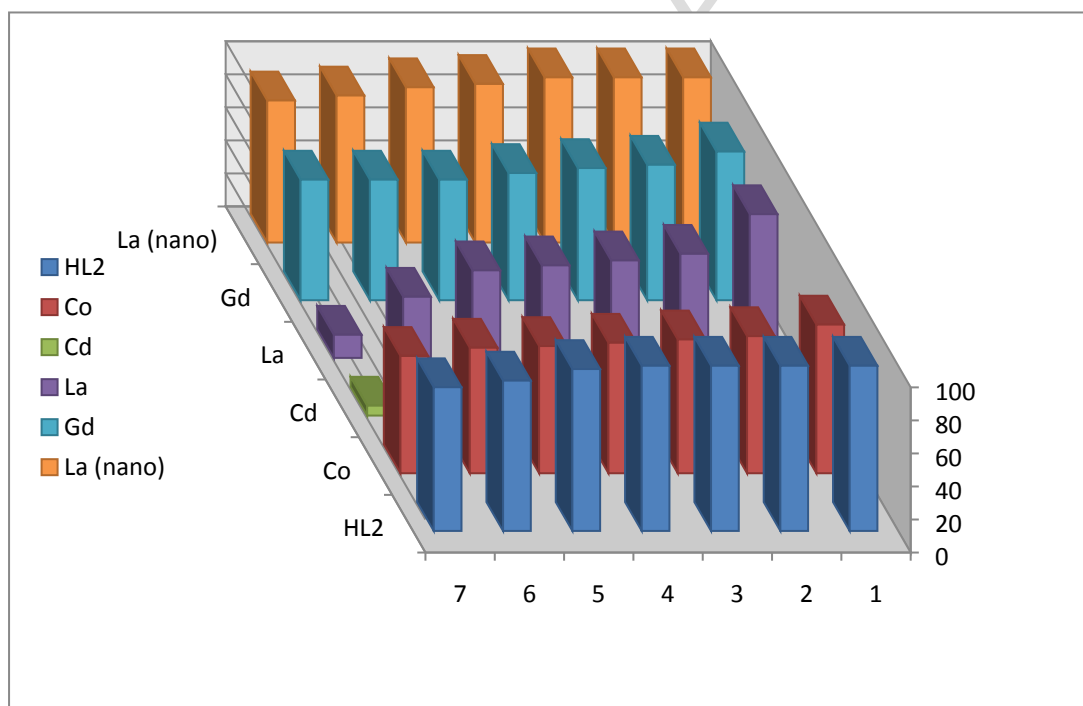
cell line	compound number	concentration( $\mu\text{g/ml}$ )						
		Cell viability%						
		10	20	30	40	60	80	100
Vero cells	HL <sup>2</sup>	100	100	100	100	98	91	87
	6	90	83	81	79	77	76	71
	7	8	8	8	7	7	7	6
	8	87	63	59	56	53	37	14
	9	90	82	80	77	73	73	73
	10	100	100	100	96	94	89	86

Table (9) : Cytotoxic effect of free ligand and its metal complexes on the viability of Caco-2 cells

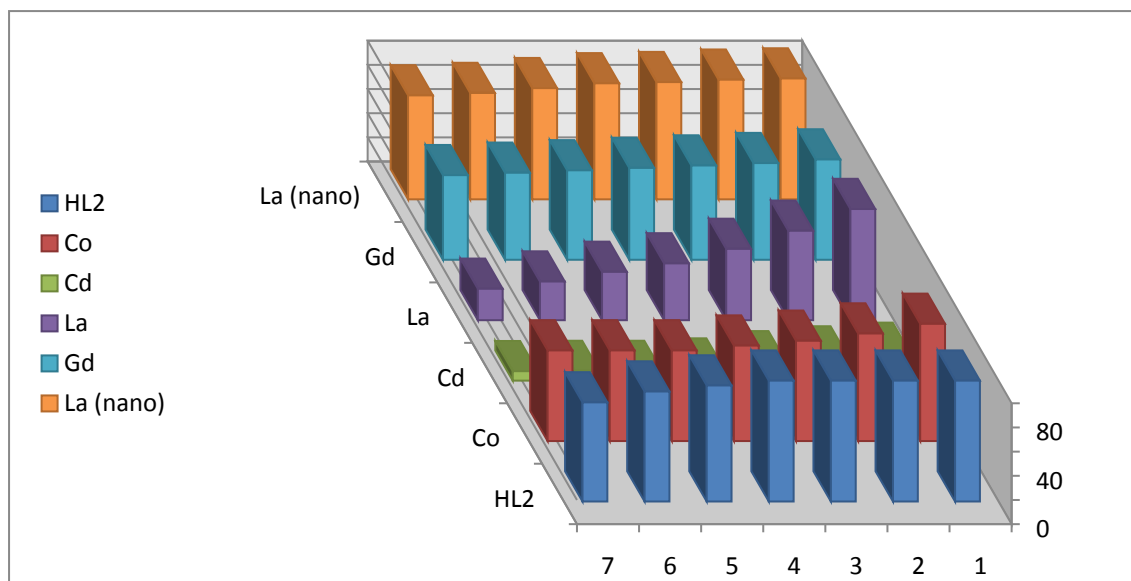
cell line	compound number	concentration( $\mu\text{g/ml}$ )						
		Cell viability%						
		10	20	30	40	60	80	100
Caco-2 cells	HL <sup>2</sup>	100	100	100	100	96	91	82
	6	97	89	83	79	75	75	75
	7	23	20	16	10	8	8	7.8
	8	92	74	59	47	40	32	26
	9	83	80	78	76	74	72	70
	10	100	99	97	96	92	88	86

Table (10) : Cytotoxic effect of free ligand and its metal complexes on the viability of MCF-7 cells

cell line	compound number	concentration( $\mu\text{g/ml}$ )						
		Cell viability%						
		10	20	30	40	60	80	100
MCF-7 cells	HL <sup>2</sup>	100	100	98	91	87	78	70
	6	91	88	81	77	69	66	61
	7	21	19	18	18	16	14	12
	8	93	90	84	72	53	39	27
	9	94	93	93	92	85	81	77
	10	96	95	94	93	91	83	67



**Fig . (18):** *In vitro* cells viability assay against different concentrations of the free ligand and its metal complexes using Vero cell lines



**Fig. (19) :** *In vitro* cells viability assay against different concentrations of the free ligand and its metal complexes using Caco-2 cell lines

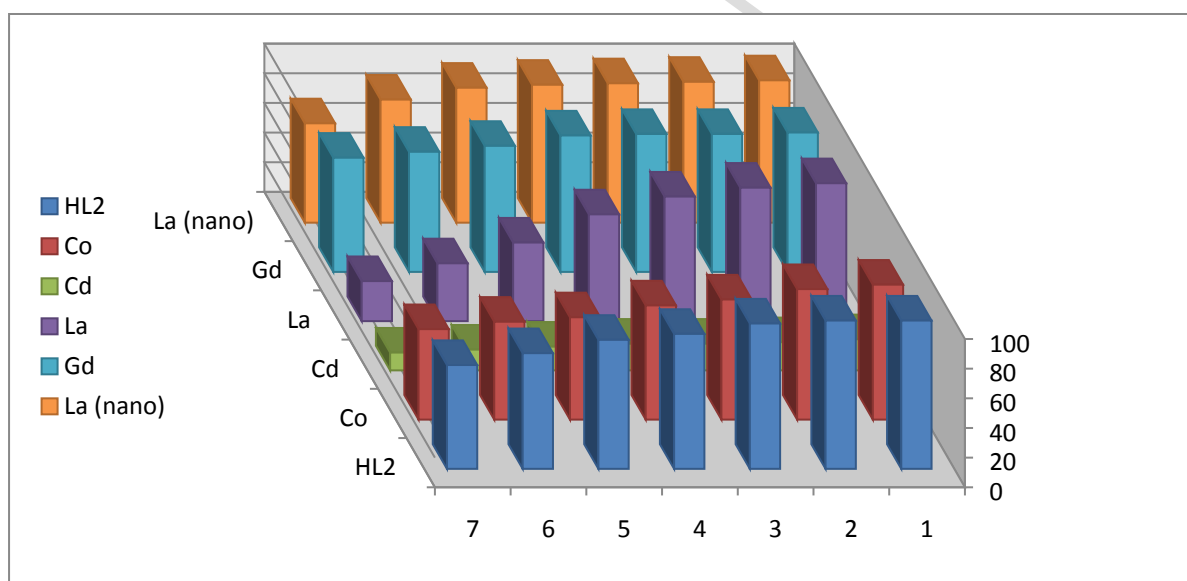


**Fig. (20) :** *In vitro* cells viability assay against different concentrations of the free ligand and its metal complexes using MCF-7 cell lines

## Conclusion

The Schiff base ligand from benzoin and 2-aminothiophenol and its metal complexes both in bulk and nano size were prepared and characterized using different techniques. The ability of the free ligand to remove different heavy metals was studied. The cytotoxicity effect of Cd(II) complexing MTT method exhibited a significant nontoxic behavior and

higher cell viability on Vero, Caco-2 and MCF-7 cells than the free ligand itself. The cytotoxicity results revealed that the Cd(II) complex could become safe to be used as anticancer agent for Vero, Caco-2 and MCF-7 cells. By examining its pharmacological activity, we were able to identify new potent and selective anticancer.

### Conflict of Interest

The authors have no conflict of interest to declare.

### References

- [1] Y. Gutha, Y. Zhang, W. Zhang and X. Jiao, *International Journal of Biological Macromolecules*, 97(2017)85-98.
- [2] E. M. S. Azzam, G. Eshaq, A. M. Rabie, A. A. Bakr, A. A. Abd-Elaal, A. E. El Metwally and S. M. Tawfik, *International Journal of Biological Macromolecules*, 89(2016)507-517.
- [3] A. Z. El-Sonbati, M. A. Diab, A. A. El-Bindary, G. G. Mohamed, Sh. M. Morgan, M. I. Abou-Dobara, S. G. Nozha, *Journal of Molecular Liquids* 215 (2016) 423-442.
- [4] N. A. El-Ghamaz, E. M. El-Menyawy, M. A. Diab, A. A. El-Bindary, A. Z. El-Sonbati, S. G. Nozha, *Solid State Sci.* 30 (2014) 44-54.
- [5] N. A. El-Ghamaz, M. A. Diab, A. A. El-Bindary, A. Z. El-Sonbati, S. G. Nozha, *Spectrochim. Acta A* 143 (2015) 200-212.
- [6] S. Medici, M. Peana, V. M. Nurchi, J. I. Lachowicz, G. Crisponi, M. A. Zoroddua, *Coord. Chem. Rev.* 284 (2015) 329.
- [7] C. E. Satheesh, P. Raghavendra Kumar, P. Sharma, K. Lingaraju, B. S. Palakshamurthy, H. Raja Naika, *Inorg. Chim. Acta* 442 (2016) 1.
- [8] M. N. Patel, C. R. Patel, H. N. Joshi, *Inorg. Chem. Commun.* 27 (2013) 51;
- [9] M. T. Kaczmarek, M. Zabizak, M. Nowak, R. Jastrzab, *Coordination Chemistry Reviews* 370, 42-54, 2018.
- [10] K. Vinay Kumar, K. Sunand, K. Ashwini, P. Suresh Kumar, S. Vishnu, Alivelu Samala, *International Journal of Applied Pharmaceutical Sciences and Research* 2017; 2(1):8-14.
- [11] Jansi Rani and Bhecter, *World Journal of Pharmacy and Pharmaceutical Sciences*, 5 (6), (2016) 895-904

- [12] H. M. Aly, R. H. Taha, N. M. El-deeb and A. Alshehri, *Inorg. Chem. Front.*, (2018), 5, 454–473.
- [13] O., Almahdy, E.M. EL-Fakharany, E. EL-Dabaa, T.B. Ng and E.M. Redwan, 2011..*Hepat. Mon.*, 11: 724–730
- [14] E.M., El-Fakharany, L. Sánchez, H.A. Al-Mehdar and E.M. Redwan, 2013. *Virolog. J.*, 10: 199
- [15] T., Mosmann, *J. Immunol. Methods* (1983), 65: 55–63
- [16] A.Z. El –Sonbati ,M.A.Diab , A.A. EL-Binary , A.M. Eldesoky , Sh. M. Morgan , *Spectrochim , Acta A* 135 (2015) 774-791 .
- [17] Ashley M Smith , Lauren E Marbella , Kathryn A Johnston , Michael J Hartmann , Scott E , *Analytical Chemistry* 87 (5) , 2771-2778 , 2015 .
- [18] M.A.A. Ali, A.M.S. Mohamad, and M.A. Hadi ,*Jornal of Kufa for chemical science* 2(1) :64-71 (2011) .
- [19] G. S. Kurdekar, M. P. Sathisha, S. Bundagumpi, N. V. Kulkarni, V.K.Revankar , and D.K.Suresh , *Med.Chem.Res.* (2012) 21:2273-2279.
- [20] A. Xavier, N.Srividhya, P.Gobu, *Indian journal of applied research*, 5 (2015).
- [21] W. Peng , H. Li, Y. Liu and S. Song, *Journal of Molecular Liquids*. 230(2017)496-504.
- [22] R. Hasanzadeh , P. N. Moghadam, N. B. Laleh and M. Sillanp , *J. Colloid Interface Sci.* 490(2017)727-746.
- [23] H. Baseri and S. Tizro, *ProcessSaf. Environ. Prot.* 109(2017) 465-477.

- A new Schiff base ligand and its metal complexes were prepared.
- La(III) complexes were prepared in bulk and nano size.
- These compounds were characterized by different physicochemical techniques.
- The ability of the free ligand to remove different heavy metals was studied
- We were able to identify new potent and selective anticancer agents